Mon. Not. R. Astron. Soc. **385,** 2136–2142 (2008) doi:10.1111/j.1365-2966.2008.12982.x

The formation of ultra-compact dwarf galaxies and nucleated dwarf galaxies

Tobias Goerdt,[1,2]★ Ben Moore,[1] Stelios Kazantzidis,[3] Tobias Kaufmann,[4] Andrea V. Macciò[5] and Joachim Stadel[1]

[1]*Institut für Theoretische Physik, Universität Zürich, Winterthurerstrasse 190, CH-8057 Zürich, Switzerland*
[2]*Racah Institute of Physics, The Hebrew University, Jerusalem 91904, Israel*
[3]*Kavli Institute for Particle Astrophysics and Cosmology, Stanford University, 2575 Sand Hill Rd, Menlo Park, CA 94025 USA*
[4]*Centre for Cosmology, Department of Physics and Astronomy, University of California, Irvine, CA 92697, USA*
[5]*Max-Planck-Institut für Astronomie, Königstuhl 17, D-69117 Heidelberg, Germany*

Accepted 2008 January 15. Received 2008 January 11; in original form 2007 October 31

ABSTRACT

Ultra-compact dwarf galaxies (UCDs) have similar properties as massive globular clusters or the nuclei of nucleated galaxies. Recent observations suggesting a high dark matter content and a steep spatial distribution within groups and clusters provide new clues as to their origins. We perform high-resolution *N*-body/smoothed particle hydrodynamics simulations designed to elucidate two possible formation mechanisms for these systems: the merging of globular clusters in the centre of a dark matter halo, or the massively stripped remnant of a nucleated galaxy. Both models produce density profiles as well as the half-light radii that can fit the observational constraints. However, we show that the first scenario results to UCDs that are underluminous and contain no dark matter. This is because the sinking process ejects most of the dark matter particles from the halo centre. Stripped nuclei give a more promising explanation, especially if the nuclei form via the sinking of gas, funnelled down inner galactic bars, since this process enhances the central dark matter content. Even when the entire disc is tidally stripped away, the nucleus stays intact and can remain dark matter dominated even after severe stripping. Total galaxy disruption beyond the nuclei only occurs on certain orbits and depends on the amount of dissipation during nuclei formation. By comparing the total disruption of cold dark matter subhaloes in a cluster potential, we demonstrate that this model also leads to the observed spatial distribution of UCDs which can be tested in more detail with larger data sets.

Key words: methods: *N*-body simulations – galaxies: formation – galaxies: star clusters.

1 INTRODUCTION

A new population of subluminous and extremely compact objects have been recently discovered in cluster and group environments (Drinkwater et al. 2000; Phillipps et al. 2001). These ultra-compact dwarf galaxies (hereafter UCDs) are dynamically distinct systems having intrinsic sizes $\lesssim$100 pc and absolute magnitudes in the *B* band in the range from -13 to -11 placing them in the lower range of dwarf galaxy luminosities (Mateo 1998). A number of different scenarios have been proposed for origin of UCDs (e.g. Evstigneeva et al. 2007, and references within): (i) they are simply very big and luminous globular clusters, (ii) they are nucleated dwarf galaxies, (iii) they are the resulting objects of the coalescence of several globular clusters, (iv) they are the remnants of stripped disc galaxies. In this work, we compare the last two scenarios.

Oh & Lin (2000), Oh, Lin & Richer (2000) as well as Fellhauer & Kroupa (2002) investigated the third formation scenario. The latter authors performed *N*-body simulations of the merging of several globular clusters and argued that the resulting object resembled a UCD. Their simulations initiated with a supercluster, an accumulation of up to 50 globular clusters, orbiting inside a host galaxy on fairly elliptical orbits and with apogalactic distances around 20 kpc. The globular clusters merged within the supercluster giving rise to an object with values for surface brightness and absolute bolometric luminosity comparable to UCDs.

The last formation scenario has been discussed in Oh, Lin & Aarseth (1995) as well as in Bekki, Couch & Drinkwater (2001, 2003). The latter authors performed numerical simulations of the dynamical evolution of nucleated dwarf galaxies orbiting inside NGC 1399 and the Fornax cluster. Adopting a plausible scaling

★E-mail: tgoerdt@phys.huji.ac.il

relation for dwarf galaxies, Bekki et al. found that the outer stellar envelope of a nucleated dwarf was totally removed by tidally stripping over the course of several passages from the central region of their host. The nucleus is so dense that it will always survive the tidal field of a group or cluster potential. By construction in the initial conditions, the size and luminosity of the remnant were similar to those observed for UCDs and the host galaxy was a Plummer model halo which has a constant density core, and therefore easy to tidally disrupt leaving behind the central nucleus which would be associated with a UCD.

The main goal of the present study is to shed light into the formation of UCDs investigating the last two formation scenarios in more detail and with more realistic initial conditions. First, we adopt the Fellhauer & Kroupa (2002) model and combine it with the cold dark matter model (CDM) paradigm. We assume that globular clusters form and subsequently orbit around dark matter haloes having masses comparable to that of the Fornax dwarf spheroidal and containing no other baryonic matter. Due to dynamical friction, these globular cluster would spiral in towards the centre of the halo. We perform collisionless *N*-body simulations of this process, and show that the object resulting from the coalescence of the globular clusters at the halo centre resembles a UCD. As we demonstrate below, the above model suffers from two major drawbacks which rule out its applicability for UCD formation.

The first issue is related to the observed high mass-to-light (M/L) ratio (between six and nine in solar units) recently reported for UCDs (Haşegan et al. 2005). One has to note here that the M/L ratio of UCDs is still debated (Micheal Drinkwater, private communication, compare Evstigneeva et al. 2007 who quote a M/L for UCDs three and five in solar units). Such high values can probably not be achieved by the above mechanism. This is because sinking globular clusters will expel most of the dark matter particles from the halo centre (El-Zant, Shlosman & Hoffman 2001; Merritt et al. 2004; Goerdt et al. 2006). If there is no dark matter in UCDs, Fellhauer & Kroupa (2006) describe a possible way to enhance the M/L ratios of UCDs through tidal interactions. The second problem with this scenario is related to the total luminosity of an UCD. At least today, dark matter haloes with a sufficient number of globular clusters to produce such bright objects are very rare (Sharina, Puzia & Makarov 1996; Böker et al. 2002).

Secondly, we examine the scenario of Bekki et al. (2001, 2003) which is based on the hypothesis that UCDs are remnants of stripped nucleated galaxies. This mechanism has also been discussed by Kazantzidis, Moore & Mayer (2003). We test this model using smoothed particle hydrodynamics (SPH) simulations of a low-mass galaxy which forms a nucleus via gas inflow to the inner ≈100 pc. Once this galaxy is placed on a critical disrupting orbit within a cluster potential, the surviving nucleus is in excellent agreement with the latest observational constraints for UCDs, including their dark matter content and spatial distribution.

The paper is organized as follows. In Section 2, we describe the globular cluster numerical simulations and compare the properties of the resulting object with those of UCDs. Section 3 contains results from the simulations of tidal stripping of disc galaxies inside a host cluster potential. Finally, in Section 4 we summarize our main conclusions.

2 THE GLOBULAR CLUSTER SIMULATIONS

The globular cluster simulations were performed with PKDGRAV2 a multistepping, parallel *N*-body TREE code (Stadel 2001). We create an NFW (Navarro, Frenk & White 1996) halo, employing the technique developed by Kazantzidis, Magorrian & Moore (2004), which has the following density profile:

$$\rho(r) = \frac{\rho_0}{r/r_\mathrm{s}\,[1+(r/r_\mathrm{s})]^2}. \quad (1)$$

In our case $\rho_0 = 242\,\mathrm{M}_\odot\,\mathrm{pc}^{-3}$ and $r_\mathrm{s} = 1.5$ kpc. The halo has a virial mass of $1.5 \times 10^9\,\mathrm{M}_\odot$. The concentration parameter is 20 which is the typical value for haloes of this initial mass. To increase mass resolution in the region of interest, we divide the halo into three shells (Zemp et al. 2007) each of which contains 10^5 particles. The innermost shell has 100 pc radius. The second shell is between 100 and 500 pc while the third shell contains the rest of the halo. The softening lengths for these shells are 1, 10 and 100 pc, respectively. This shell model allows us to resolve the detailed kinematics within the central few parsecs whilst retaining the global structure of the halo out to its virial radius of 29.39 kpc.

We use 10 globular clusters consisting of 10^5 particles and being represented by the King model (King 1966; Michie 1963; Michie & Bodenheimer 1963)

$$\rho(\Psi) = \rho_1 \exp\left(\frac{\Psi}{\sigma^2}\right) \mathrm{erf}\left(\frac{\sqrt{\Psi}}{\sigma}\right) - \rho_1 \sqrt{\frac{4\Psi}{\pi\sigma^2}}\left(1+\frac{2\Psi}{3\sigma^2}\right). \quad (2)$$

Each globular cluster is constructed with a $W_0 = \Psi(0)/\sigma^2$ parameter of 6, a total mass of $4.2 \times 10^5\,\mathrm{M}_\odot$, a central velocity dispersion of $11\,\mathrm{km\,s}^{-1}$ and an absolute magnitudes of -8.5, assuming a M/L ratio of 2 (Böker et al. 2004; Walcher et al. 2005). We use 1 pc for its gravitational softening length. The 10 globular clusters are initially distributed within the halo between 20 and 1000 pc. They are spatially distributed according to $\rho\,(r) \propto r^{-4}$, which is in agreement with observations of globular cluster populations in dwarf galaxies (Sharina, Puzia & Makarov 1996). We randomly place the globular clusters on circular orbits (We also tried different orbital and spatial distributions including r^{-3} and r^0 with similar results as in the standard r^{-4} case.).

The dwarf halo which contained the globular clusters was placed on a static NFW potential which corresponds to a cluster halo with virial mass of $M_\mathrm{vir} = 10^{14}\,\mathrm{M}_\odot$ and concentration of $c = 6$. The halo was placed on an initial distance of 100 kpc from the centre of the potential and was given a velocity of $650\,\mathrm{km\,s}^{-1}$, respectively. These values result to an eccentric orbit with an apocentre of 500 kpc. For a second simulation, we put 50 of these globular cluster in the aforementioned halo and let them spiral into the centre. This second simulation identical to the first one, just with 50 instead of 10 globular clusters.

All 10 globular clusters in our first simulation merge to a single object within 0.4 Gyr. The associated time-scale of this evolution can be calculated using the Chandrasekhar dynamical friction formula (Chandrasekhar 1943):

$$\frac{\mathrm{d}r}{\mathrm{d}t} = -\frac{4\pi \ln\Lambda(r)\rho(r)G^2 M_\mathrm{GC} r}{v_\mathrm{c}^2(r)\mathrm{d}\left[r\,v_\mathrm{c}(r)\right]/\mathrm{d}r}\left\{\mathrm{erf}\left[\frac{v_\mathrm{c}(r)}{\sqrt{2}\sigma(r)}\right] - \frac{2v_\mathrm{c}(r)}{\sqrt{2\pi}\sigma(r)}\exp\left[\frac{-v_\mathrm{c}^2(r)}{2\sigma^2(r)}\right]\right\}, \quad (3)$$

where $v_\mathrm{c}(r)$ is the circular speed at radius r, $\ln\Lambda(r)$ is the Coulomb logarithm, which we assume to be 4.0, M_GC is the mass of one globular cluster. $\rho(r)$ is the density of the dark matter halo at radius r according to equation (1) and $\sigma(r)$ is the one-dimensional velocity dispersion of the halo. Solving this equation numerically gives

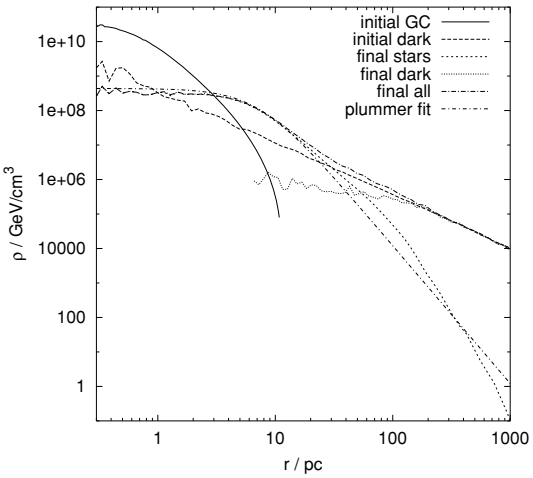

Figure 1. The different density profiles of the UCD and the corresponding dark matter distributions, after the 10 globular clusters merged, but before and after it has been put into an external potential. On top of the density profile of the final stellar distribution, we show the best-fitting plummer model.

$t_{\rm fric} = 0.4\,$Gyr, which is very similar to the value we directly get from the simulation.

The central compact object which results from the coalescence of the globular clusters has a three-dimensional density profile which is shown in Fig. 1. The profile is very similar to ones derived from observations (De Propris, Phillipps & Drinkwater 2005) as well as previous simulations (cf. fig. 5 in Fellhauer & Kroupa 2002). The density profile of the baryonic matter only (i.e. just the material, which has been in the original globular clusters) can be well fitted with a Plummer model (Plummer 1911):

$$\rho(r) = \frac{3M}{4\pi b^3}\left(1+\frac{r^2}{b^2}\right)^{-5/2}. \quad (4)$$

In our case, $M = 1.45 \times 10^6\,{\rm M}_\odot$ and $b = 7.26\,$pc. The resulting object has a half-mass radius of 25 pc and a central velocity dispersion of $20\,{\rm km\ s^{-1}}$. The projected surface density profile can be seen in Fig. 2. The fit is good in the inner parts and reasonable in the outer parts. The equation for the fit has been found by Evans & An (2005):

$$\Sigma(r) = \frac{A}{\pi\left(1+r^2/c^2\right)^2}. \quad (5)$$

Our fit gives $A = 3.3 \times 10^4\,{\rm M}_\odot\,{\rm pc}^{-2}$ and $c = 8.7\,$pc. It looks fairly similar to observations and previous simulations [cf. fig. 5 in Haşegan et al. (2005) or fig. 6 in Fellhauer & Kroupa (2002)]. If we assume a M/L ratio of 3, we expect an absolute visual magnitude of -11 for the final object. For comparison, a typical UCDs found in Fornax have a central velocity dispersion of $22\,{\rm km\ s^{-1}}$, an absolute magnitude of -12 and a half-mass radius of 25 pc (Drinkwater et al. 2003; Haşegan et al. 2005). In order to form this system by merging globular clusters, one would need to consider many more globulars to reach the observed luminosity. This turns out to be a crucial point of this formation scenario because the presence of more than 10 globulars in such a halo is extremely rare (Sharina, Puzia & Makarov 1996).

In our second simulation, the 50 globular clusters merged completely within a few million years. The resulting object had a central velocity dispersion of $37.3\,{\rm km\ s^{-1}}$ and an absolute magnitude of -12.75, assuming a M/L ratio of 3. Its position is marked in Fig. 3 and roughly matches a UCD.

Interestingly, all dark matter particles are expelled from the core of the final object and the inner initial cusp has been turned into a nearly constant density core. Indeed, in our 10 globular cluster simulation not even a single dark matter particle is found within the inner 5 pc. This effect has been discussed in more detail in Read et al. (2006) and constitutes the second reason for excluding the merging of globular clusters as a possible formation mechanism for UCDs. In other words, the observed M/L ratio cannot possibly be reached without dark matter. Only if the initial globular clusters contained cuspy dark matter distributions would such a scenario stand a chance of working, however current observations do not support this idea in the galactic globular clusters.

Keeping in mind the observational uncertainty of the M/L ratios of UCDs, the mechanism proposed by Fellhauer & Kroupa (2006) to enhance the M/L ratio of UCDs as well as resolution limits and other shortcomings of properly determining the M/L ratio of our simulations in the next section, the reader should note that the major

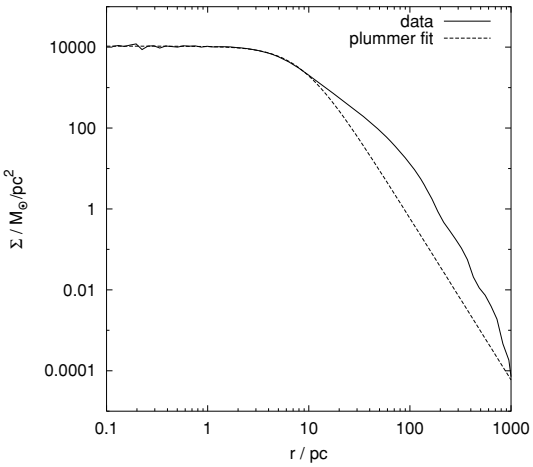

Figure 2. Projected surface density profile of the UCD, after the 10 globular clusters merged, but before it has been put into an external potential. The profile of the luminous matter together with the best-fitting plummer model is plotted.

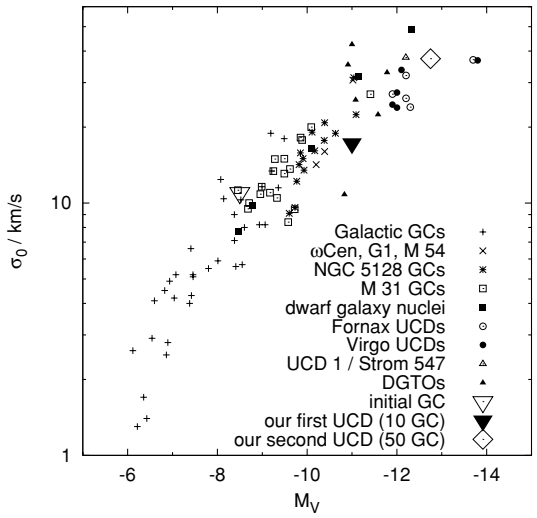

Figure 3. Central velocity dispersion versus absolute visual magnitude for various stellar systems. Observations are plotted together with the results from our simulations. Data taken from Haşegan et al. (2005); Evstigneeva et al. (2007), and references therein.

issue and stronger argument against this formation scenario is the total central luminosity.

3 ARE UCDS STRIPPED DISC GALAXIES?

The second scenario we consider for the formation of UCDs is that they are the remnants of stripped disc galaxies. For the numerical experiments performed in this section, we build galaxy models using the following procedure. First, we set up a spherical equilibrium NFW halo with structural parameters consistent with predictions of the standard ΛCDM model (Kazantzidis et al. 2004). We include a gaseous component of mass equal to a fraction f_b of the total halo mass. The gas has originally the same radial distribution and a temperature profile such that it is in hydrostatic equilibrium for an adiabatic equation of state (EOS).

The gas component has a specific angular momentum distribution and spin parameter consistent with values found for dark matter haloes within cosmological *N*-body simulations (Bullock et al. 2001; Macciòet al. 2007). We constructed a dark plus gaseous halo model with parameters that are expected to produce discs similar to the Local Group galaxy M33 which has a small dense stellar nucleus. The model parameters were: $M_{\rm vir} = 5 \times 10^{11}\,{\rm M}_\odot$, $r_{\rm vir} = 167$ kpc, $v_{\rm vir} = 115$ km s^{-1}, $c = 6.2$, baryonic fraction $f_b = 6$ per cent and spin parameter $\lambda = 0.1$.

The value of the concentration may seem a little bit low, when comparing it to the results of Macciòet al. (2007) but it is the best fit for the M33 galaxy (Corbelli 2003) which is the possible prototype progenitor for UCDs, we want to test here. The value of the spin parameter is what one gets from cosmological dark matter simulations. This net spin results from adding many large, almost randomly oriented angular momenta of individual dark matter particles. Uniformly rotating gas haloes are normally not observed in cosmological simulations, gas is accreted pretty much like the dark matter, leading to random, large bulk motions and turbulence (Wise & Abel 2007). So one has to note here that this setup is designed to produce cored discs for the subsequent experiments and not necessarily an attempt to follow disc and core formation realistically.

The hot gaseous halo is resolved with 2×10^6 particles of equal mass $\sim 2 \times 10^4\,{\rm M}_\odot$. We sampled the dark matter halo with 2.2×10^6 particles having variable masses with the resolution increasing towards the centre of the system (Zemp et al. 2007). With a single-particle model one would need about 10 million particles to reach a comparable resolution in the central region. This allows us to simulate the central dark matter cusp with softening of 100 pc (this is the same for all dark matter and gas particles) and particle mass of $\sim 4.4 \times 10^4\,{\rm M}_\odot$. The detailed description of the initial conditions and results of the evolution of the disc are presented in Kaufmann et al. (2006) and Kaufmann et al. (2007).

We use the parallel TREE+SPH code GASOLINE (Wadsley, Stadel & Quinn 2004), which is an extension of the pure *N*-Body gravity code PKDGRAV developed by Stadel (2001). It uses a 32 particles smoothing kernel and an artificial viscosity which is the shear-reduced version (Balsara 1995) of the standard Monaghan (1992) artificial viscosity. GASOLINE uses a spline kernel with compact support for the softening of the gravitational and SPH quantities. The energy equation is solved using the asymmetric formulation, which is shown to yield very similar results compared to the entropy conserving formulation but conserves energy better (Wadsley et al. 2004). The code includes radiative cooling for a primordial mixture of helium and (atomic) hydrogen. Because of the lack of molecular cooling and metals, the efficiency of our cooling functions drops rapidly below 10 000 K, but we adopt a temperature floor of $T_f = 15\,000$ K,

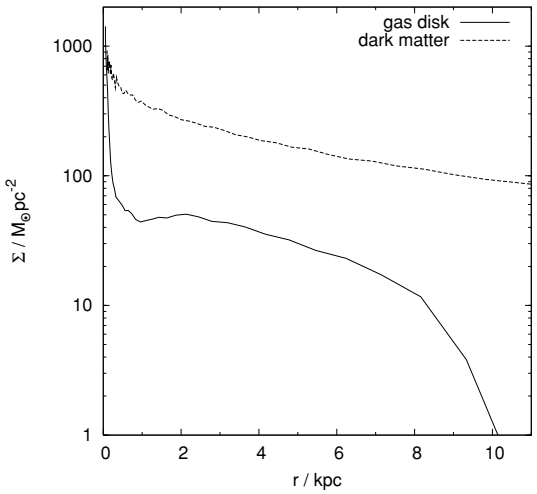

Figure 4. The logarithmic surface density of the M33 gas disc is plotted after 2.5 Gyr. The nucleus in the centre is clearly visible. The dark matter distribution is plotted on top for comparison.

to crudely mimic the effect of heating sources such as supernovae explosions and radiation (e.g. ultraviolet) backgrounds. These simulations were performed without star formation. We do not expect them to suffer from the SPH problems pointed out by Agertz et al. (2007) because for the disc-forming part of the simulations, we are adopting a large temperature floor and do not aim to simulate the actual multiphase ISM, where the problems would occur. The gas cools slowly to form a disc and stars are formed at a rather low threshold, therefore there is problem with our simulations (Oscar Agertz, private communication). For a detailed discussion on the performance of SPH for the stripping part of the simulations, we defer the interested reader to McCarthy et al. (2008).

Due to cooling the hot gas, halo loses its hydrostatic equilibrium quite quickly. An inner gaseous disc rapidly forms out of cooling gas coming from a nearly spherical region close to the halo centre (within ∼10 kpc). After 2.5 Gyr of evolution, the disc attains a near exponential surface density profile over a large fraction of its extent, except within a few 100 pc from the centre, where gas inflows along an inner bar produce a dense nucleus which can be seen in Fig. 4.

The nucleus has a mass of $\sim 3 \times 10^7\,{\rm M}_\odot$, which is ∼0.6 per cent of the total disc. Central dense stellar nuclei have been seen in several late-type spiral galaxies, for example, in M33 (Regan & Vogel 1994), but also in other late-type spirals (Carollo, Stiavelli & Mack 1998; Carollo 1999). Recent observations by Ferrarese et al. (2006) show that they are observed in 50–80 per cent of low- and intermediate-luminosity galaxies.

We put the galaxy into the same artificial NFW potential resembling the Virgo cluster that we used before. We start with the disc at pericentre, 100 kpc far from the centre of the static potential, and give it a perpendicular velocity of 260 km s^{-1}, such that it should reach an apocentre at 30 kpc. The plane of the disc is tilted by 45° with respect to the plane of the orbit. On this orbit, the outer galactic halo and gas are quickly stripped from the nucleus.

The resolution of our hydrodynamic simulation is not sufficient to allow a meaningful comparison with the observations. However, the half-light radius, luminosity and dark matter content all agree well with observations up to the given resolution limits (see Fig. 5), the M/L ratio within the optical radius (∼50 pc) is about 4. and the UCD is dark matter dominated up to the resolution limit.

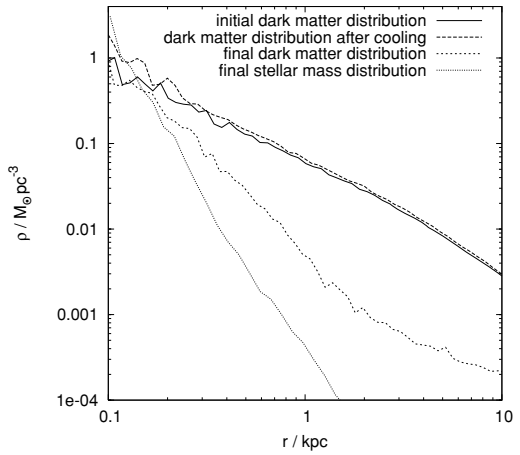

Figure 5. The dark matter distributions of the disc model in various stages of its evolution, together with the final baryonic (stellar) mass distribution.

3.1 Defining the critical disruption zone and the affects of baryons on survival versus disruption

If the orbit of the galaxy does not penetrate the centre of the cluster then the disc would not be stripped and the object would not be classified as a UCD. If the progenitors are nucleated discs which are tidally transformed into nucleated spheroidals d$E(N)$ via galaxy harassment (Moore et al. 1996) then we might expect a transition region from central UCDs to outer d$E(N)$. Since UCDs are all located close to the centres of clusters and groups, this allows us to explore the conditions under which complete disruption occurs and how that is affected by the amount of dissipation (steepening of the central potential).

In what follows, we performed an extensive set of simulations to identify the orbits on which the disc galaxy is completely stripped and on which it remains intact. The first case would correspond to a UCD and the second to a d$E(N)$. The central potential of the SPH galaxy is deepened significantly due to dissipation. The object will be harder to completely disrupt as compared to the initial dark matter halo of the model, for example. We therefore make a systematic study of the orbits that lead to disruption versus survival for the nucleated M33 galaxy model and for the initial uncompressed dark matter halo – the latter simulations define the optimum scenario for complete disruption.

These simulations all start at their respective apocentres and run for the same physical time (5 Gyr) in the cluster potential, and explore different orbital apocentres and pericentres. If stripping of disc galaxies is the correct mechanism for forming UCDs and d$E(N)$, there must be a very sudden transition between these two cases. This is because we do not observe an intermediate object with features lying in between these very distinct two types of galaxies.

Fig. 6 presents surface brightness profiles of the disc galaxy after orbiting the static cluster potential for 5 Gyr on various orbits. A sudden transition is clearly seen in this plot: almost two orders of magnitude in surface brightness lie between the (150−30) and the (125−25) orbit at the radii of interest, so the disc either survives or is completely disrupted.

Fig. 7 presents a scatter plot of apocentres versus pericentres for all cases, we simulated along with indications about the fate of the orbiting system. The dividing line between disrupted and surviving discs is given by

$$r_{\rm peri} = A r_{\rm apo} + B \quad (6)$$

with A = −0.32 and B = 68.

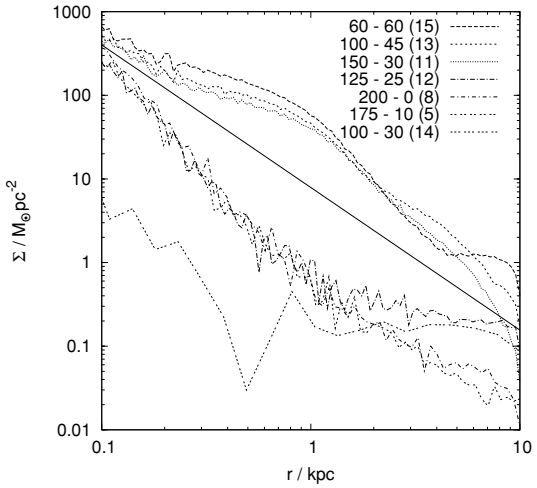

Figure 6. Surface brightness profiles of the stripped disc after orbiting an artificial Virgo cluster potential for 5 Gyr. The numbers next to the hyphen in the legend give the apo and pericentres of the various orbits in kpc and the numbers within the brackets give the number of orbits which were completed during the 5 Gyr. The solid line indicates the dividing line between survival and disruption.

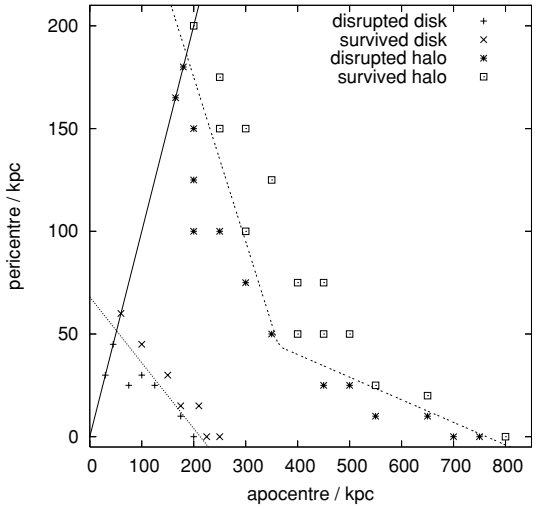

Figure 7. Disrupted and non-disrupted gas discs and dark matter halo nuclei as a function of apo and pericentre for all the disc and the dark matter only simulations we have done. The solid line is the bisector and the two dotted ones are the dividing lines between disruption and survival.

We also repeated the above stripping experiments with the dark matter halo only without the gas disc. Results of these experiments are included in Fig. 7. In this case, the transition is not as sudden as in the disc case therefore we define a halo to be completely disrupted, if less than 0.1 per cent of the virial mass is still bound. Defining complete disruption by the bound mass getting below a certain threshold is the most objective way to do so. The value of 0.1 per cent, may seem arbitrary, but it is actually the value, which gave the most convincing values for the given resolution and algorithm. To estimate the mass which is still bound we used the group finding algorithm SKID (Stadel 2001). There is a clear separation between survival and disruption that depends only on the apocentre and pericenter. The theoretical explanation for the orbits that lead to complete disruption is fairly intricate and will be

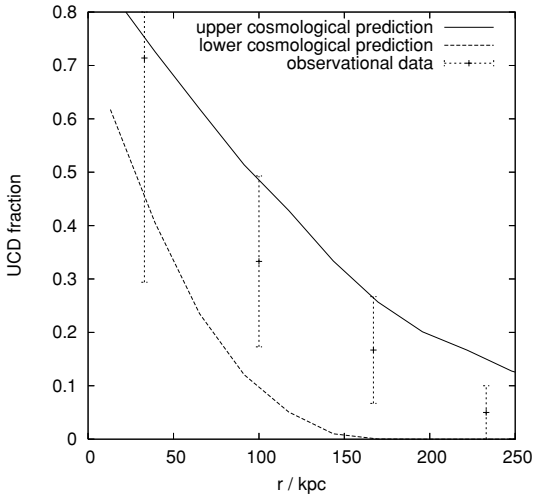

Figure 8. The ratio of the number of UCDs to the number of progenitors, which is sum of the number of UCDs and the number of d$E(N)$s, as a function of radius. The upper cosmological prediction comes from the disruption simulations using the pure dark matter subhalo whilst the lower cosmological prediction comes from the SPH simulations with the dissipated gas disc. Observational data are taken from Jones et al. (2006).

discussed in a later paper. The dividing line between disrupted and surviving haloes is given roughly by two straight lines:

$$r_{\rm peri} = Ar_{\rm apo} + B$$
$$r_{\rm peri} = Cr_{\rm apo} + D \quad (7)$$

with $A = -0.11$, $B = 84.0$, $C = -0.8$, $D = 335.0$, with the transition between them at $r = (D - B)/(A - C) \sim 370$ kpc.

Given these empirically determined survival/disruption curves, we can sample orbits from a cosmological cluster mass CDM halo and determine the expected radial profile of completely disrupted haloes (UCDs) in each of these two cases. From the cosmological simulation, we chose the one cluster which was not perturbed by neighbouring clusters, had only a single nucleus and came closest in $M_{\rm vir}$ and $r_{\rm vir}$ to the Virgo cluster.

We evolved the halo for 5 Gyr and binned all particles according to their projected distance from the centre at the last simulation output. For each bin, we determined the fraction of particles whose orbits during the 5 Gyr of evolution lies below the respective dividing line in Fig. 7. The orbits have been determined in a way that the pericentre is the closest point the particle gets to on all snapshot and the apocentre is the furthest point. In Fig. 8, this fraction is then compared to its observed counterpart in nature. This is the fraction of the number of UCDs to the number of progenitors, which is the sum of the number of UCDs and the number of d$E(N)$s, so

$$f_{\rm UCD} = \frac{n_{\rm UCD}}{n_{\rm progenitor}} = \frac{n_{\rm UCD}}{n_{\rm UCD} + n_{{\rm d}E(N){\rm s}}}. \quad (8)$$

Results from the pure dark matter stripping experiments correspond to the upper cosmological prediction (The final radial distribution of UCDs is more extended since the dark matter halo is not compressed due to dissipation and disrupts at larger clustercentric radii). The SPH disc galaxy stripping simulations correspond to the lower cosmological prediction. We have to remind the reader again that our prototype progenitor was M33 that has a concentration, which might look a bit low according to Macciòet al. (2007). Therefore, the subhalo disruption and the UCD fractions might be slightly overestimated. However, one could image the progenitor being heavier, therefore less-concentrated and thus showing the same disruption behaviour as the haloes we present. Unfortunately, we did not have the computational resources to explore parameter space any further. The observational data have been obtained in the following way. The projected distances of UCDs and d$E(N)$s in arcsec (Jones 2006) are converted into kpc assuming that the Virgo and Fornax cluster lie at distances of 16 and 20 Mpc, respectively. In a ΛCDM universe, haloes are approximately self similar so we can compare results by scaling everything with respect to the virial radius. After rescaling, we binned the occurrence of the UCDs and d$E(N)$s according to their rescaled projected distance to their mutual galaxy cluster centre into common bins. The content of each bin is associated with a Poissonian error. Finally, we divide the number of UCDs in each bin by the sum of the numbers of UCDs and d$E(N)$s and propagate the errors accordingly. From comparing our two cosmological prediction with the data, we conclude that (i) both UCDs and d$E(N)$s originate from the same progenitors and (ii) this progenitor must have properties in between the disc galaxy and the pure dark matter halo we adopted in our simulations. One must bear in mind though that we only have position data for 15 UCDs from the literature. None the less, and limitations notwithstanding, our cosmological predictions agree well with the data but further observations will allow a better test of this model.

4 CONCLUSIONS

UCDs have similar properties as massive globular clusters or the nuclei of nucleated galaxies. Recent observations of a high dark matter content and their steep spatial distribution within groups and clusters give us new clues as to their origins. We perform N-body simulations and compare two possible mechanisms for their formation: the merging of globular clusters in the centre of a dark matter halo, or the massively stripped remnant of a nucleated galaxy. Our simulations reveal that a swarm of 10 as well as one of 50 globular clusters born in a Fornax dwarf spheroidal size, dark matter halo will normally evolve to an object, which has the same density profile as an UCD. We performed a second series of simulations in which a disc galaxy experiences mass-loss processes inside a cluster environment. The disc is entirely stripped and the remaining nucleus exhibits all of the observed UCD properties. Both models produce density profiles as well as the half-light radii that can fit the observational constraints very well.

However, we show that the first scenario produces UCDs that are underluminous and contain no dark matter – the sinking process ejects most of the dark matter particles from the halo centre. The stars, which consist the globulars, would replace the dark matter particles and expel them from the centre of the halo (El-Zant et al. 2001; Merritt et al. 2004) lowering the M/L ratio beyond observational constraints (Haşegan et al. 2005). The other drawbacks of this model are that it is very unlikely to have so many globular cluster in a halo of that size. It becomes apparent in Fig. 3 that it is not sufficient to merge only 10 globulars: approximately 50 are necessary. However, such a halo may not exist (Sharina, Puzia & Makarov 1996).

Stripped nuclei give a more promising explanation, especially if the nuclei form via the sinking of gas, funneled down inner galactic bars, since this process enhances the central dark matter content. Even when the entire disc is stripped away, the nucleus remains intact and can be dark matter dominated. The total disruption of the galaxy beyond the nuclei only occurs on certain orbits and depends on the amount of dissipation during nuclei formation. By comparing the total disruption of CDM subhaloes in a cluster potential, we show that this model also leads to the observed spatial distribution

of UCDs. This scenario can be tested in more detail with larger data sets.

ACKNOWLEDGMENTS

It is a pleasure to thank Monica Haşegan, Bryn Jones, Katya Evstigneeva and Michael Drinkwater for their kindness to send us data to help with our figures. SK is supported by a Kavli Institute for Particle Astrophysics and Cosmology Postdoctoral Fellowship at Stanford University. All computations were made on the zBox and zBox2 supercomputers at the University of Zürich. Special thanks to Doug Potter for bringing zBox2 to life. TG is a Golda Meir fellow.

REFERENCES

Agertz O., Moore B., Stadel J. et al., 2007, MNRAS, 380, 963
Balsara D. S., 1995, J. Comput. Phys., 121, 357
Bekki K., Couch W. J., Drinkwater M. J., 2001, ApJ, 552, 105
Bekki K., Couch W. J., Drinkwater M. J., 2003, MNRAS, 344, 399
Böker T., Laine S., van der Marel R. P., Sarzi M., Rix R. W., Ho L. C., Shields J. C., 2002, AJ, 123, 1389
Böker T., Sarzi M., McLaughlin D. E., van der Marel R. P., Rix H. W., Ho L. C., Shields J. C., 2004, AJ, 127, 105
Bullock J. S., Dekel A., Kolatt T. S., Kravtsov A. V., Klypin A. A., Porciani C., Primack J. R., 2001, ApJ, 555, 240
Carollo C. M., 1999, ApJ, 523, 566
Carollo C. M., Stiavelli M., Mack J., 1998, AJ, 116, 68
Chandrasekhar S., 1943, ApJ, 97, 255
Corbelli E., 2003, MNRAS, 342, 199
De Propris R., Phillipps S., Drinkwater M. J., 2005, ApJ, 623, 105
Drinkwater M. J., Jones J. B., Gregg M. D., Phillipps S., 2000, PASA, 17, 227
Drinkwater M. J., Gregg M. D., Hilker M., Bekki K., Couch W. J., Ferguson H. C., Jones J. B., Phillipps S., 2003, Nat, 423, 519
El-Zant A., Shlossman I., Hoffman Y., 2001, ApJ, 560, 636
Evans N. W., An J., 2005, MNRAS, 360, 492
Evstigneeva E. A., Gregg M. D., Drinkwater M. J., Hilker M., 2007, AJ, 133, 1722
Fellhauer M., Kroupa P., 2002, MNRAS, 330, 642
Fellhauer M., Kroupa P., 2006, MNRAS, 367, 1577
Ferrarese L. et al., 2006, ApJ, 644, 21
Goerdt T., Moore B., Read J. I., Stadel J., Zemp M., 2006, MNRAS, 368, 1073
Haşegan M. et al., 2005, ApJ, 627, 203
Hernquist L., 1990, ApJ, 356, 359
Hilker M., Infante L., Viera G., Kissler-Patig M., Richtler T., 1999, A&AS, 134, 75
Jones J. B. et al., 2006, AJ, 131, 312
Kazantzidis S., Magorrian J., Moore B., 2004, ApJ, 601, 37
Kazantzidis S., Moore B., Mayer L., 2003, preprint (astro-ph/0307362)
Kaufmann T., Mayer L., Wadsley J., Stadel J., Moore B., 2006, MNRAS, 370, 1612
Kaufmann T., Mayer L., Wadsley J., Stadel J., Moore B., 2007, MNRAS, 375, 53
King I. R., 1966, AJ, 71, 64
McCarthy I. G., Frenk C. S., Font A. S., Lacey C. G., Bower R. G., Mitchell N. L., Balogh M. L., Theuns T., 2008, MNRAS, 383, 593
Macciò A. V., Dutton A. A., van den Bosch F. C., Moore B., Potter D., Stadel J., 2007, MNRAS, 378, 55
Mateo M. L., 1998, ARA&A, 36, 435
Merritt D., Piatek S., Zwart S. P., Hemsendorf M., 2004, ApJ, 608, 25
Michie R. W., 1963, MNRAS, 125, 127
Michie R. W., Bodenheimer P. H., 1963, MNRAS, 126, 269
Moore B., Katz N., Lake G., Dressler A., Oemler A., 1996, Nat, 379, 613
Moore B., Quinn T., Governato F., Stadel J., Lake G., 1999, MNRAS, 310, 1147
Monaghan J. J., 1992, ARA&A, 30, 543
Navarro J. F., Frenk C. S., White S. D. M., 1996, ApJ, 462, 563
Oh K. S., Lin D. N. C., 2000, ApJ, 543, 620
Oh K. S., Lin D. N. C., Aarseth S. J., 1995, ApJ, 422, 142
Oh K. S., Lin D. N. C., Richer H. B., 2000, ApJ, 531, 727
Phillipps S., Drinkwater M. J., Gregg M. D., Jones J. B., 2001, ApJ, 560, 201
Plummer H. C., 1911, MNRAS, 71, 460
Read J. I., Goerdt T., Moore B., Pontzen A. P., Stadel J., Lake G., 2006, MNRAS, 373, 1451
Regan M. W., Vogel S. N., 1994, ApJ, 434, 536
Sharina M. E., Puzia T. H., Makarov D. I., 2005, A&A, 442, 85
Stadel J., 2001, PhD thesis, Univ. Washington
Wadsley J., Stadel J., Quinn T., 2004, New Astron., 9, 137
Walcher C. J. et al., 2005, ApJ, 618, 237 [Erratum-ibid, 2005, 635, 741]
Wise J. H., Abel T., 2007, ApJ, 665, 899
Zemp M., Moore B., Stadel J., Carollo C. M., Madau P., 2007, MNRAS, submitted (arXiv:0710.3189)

This paper has been typeset from a TEX/LATEX file prepared by the author.